Mass transfer coefficients for water at silica surfaces evaluated on the basis of literature data
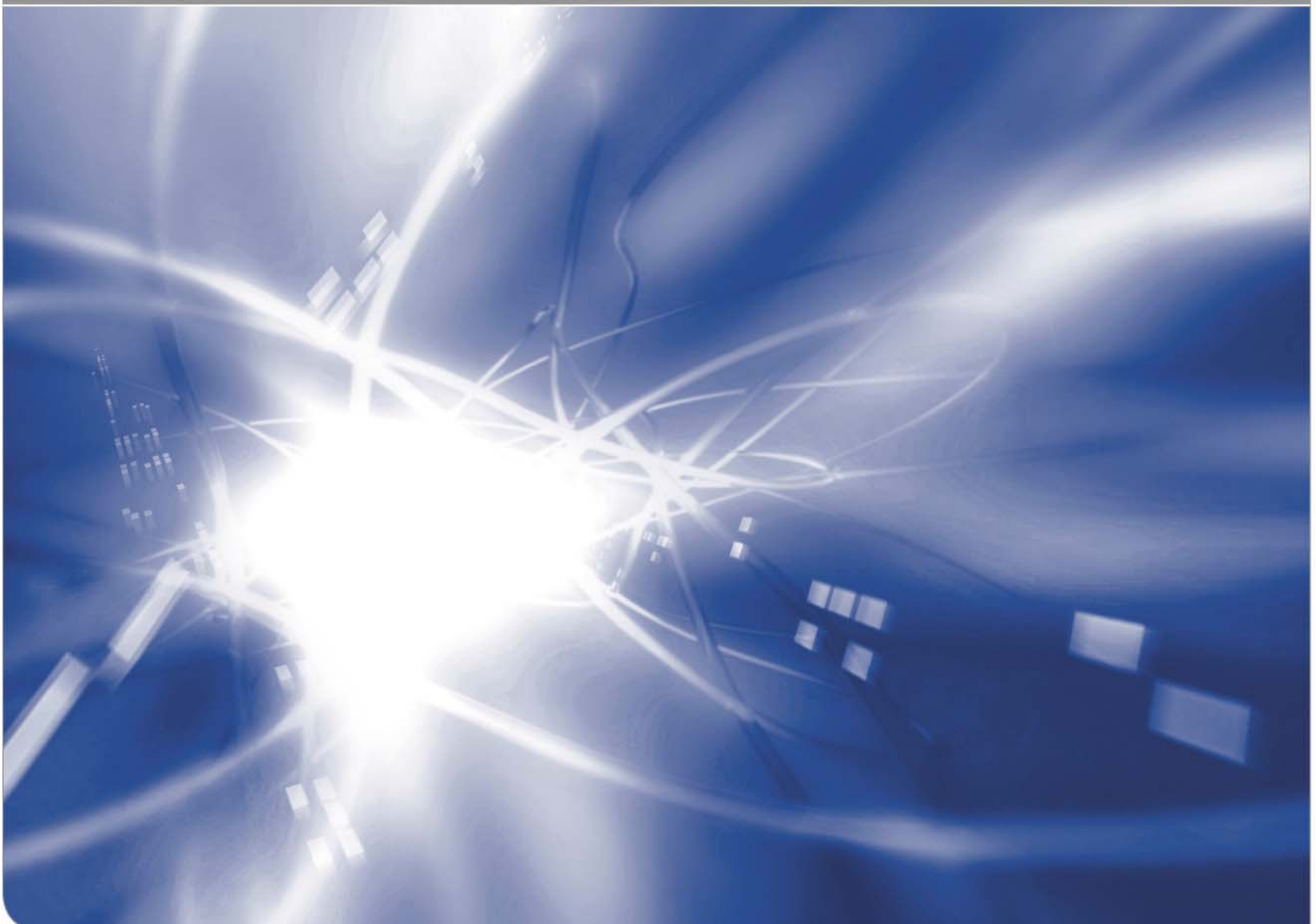
Theo Fett, Günter Schell, Claudia Bucharsky

Institute for Applied Materials

Abstract

In a number of earlier reports on the uptake of water at silica surfaces, we studied the time dependence of the water concentration. Measurements from literature could be described by a mass transfer surface condition for diffusion that hinders free water penetration from a water vapour environment into silica. So far, the related mass transfer coefficient has been determined predominantly from water uptake measurements.

Experimental data from literature allowed an evaluation of the coefficient $h/\sqrt{D}$ (h = mass transfer coefficient, D = diffusivity of water in silica). In this report, we can share explicit data on h.

For two grades of Suprasil we obtained Arrhenius-dependencies between h and temperature.

Contents

1. Importance of the mass transfer coefficient for diffusion problems

At a silica surface exposed to a water vapour environment, there are simultaneously increased molecular and hydroxyl water concentrations observed [1], Fig. 1, that can be described by a diffusion surface condition of

$$\frac{dC}{dz} = \frac{h}{D}(C - C_0) \quad \text{at} \quad z=0, \tag{1}$$

where D is the water diffusivity, C_0 the asymptotically reached water concentration, z the depth coordinate, and h a parameter that describes reduced water entrance [2, 3]. The phenomenological parameter h in (1) may be interpreted as a *reaction parameter* for a slow surface reaction that limits the entrance of molecular water species as suggested by Doremus [2] without specifying the surface reaction.

On the other hand, a simple phenomenological description is possible by assuming that a layer with very high hydroxyl water concentration exists, acting as a barrier to the transport of water across the surface of the glass (for a physical description of such a barrier see [3]). Such a barrier gives rise for a finite *mass transfer coefficient* for diffusion, which slows the passage of water into the glass. Each of the assumptions yields the same set of mathematical equations.

Under the boundary condition (1) Carslaw and Jaeger (Section 2.7 in [4]) showed that the concentration profile, $C(z)$ resulting for a semi-infinite body is given by

$$C(z, t)/C_0 = \text{erfc}\left[\frac{z}{2\sqrt{Dt}}\right] - \exp\left[\frac{h}{D}z + \frac{h^2}{D}t\right]\text{erfc}\left[\frac{z}{2\sqrt{Dt}} + h\sqrt{\frac{t}{D}}\right] \tag{2}$$

Especially, the concentration at the surface $z \to 0$ reads as a function of time t [4]

$$C(0, t)/C_0 = 1 - \exp\left[\frac{h^2}{D}t\right]\text{erfc}\left[h\sqrt{\frac{t}{D}}\right], \tag{3}$$

For an application of the preceding equations it has to be assumed that the ratio of hydroxyl to molecular water $k=[\equiv\text{SiOH}]/[\text{H}_2\text{O}]$ is sufficiently independent of time t, i.e. the water/silica reaction at the surface is in equilibrium.

2 Determination of the mass transfer coefficient

2.1 Measurements from literature

Experimental data are available in the literature that allow an evaluation of the coefficient $h/\sqrt{D}$. Uptake measurements by Wakabayashi and Tomozawa [5] on Suprasil W, type-IV glass were used in [3] and [6] to determine the parameter $h/\sqrt{D}$ by fitting the

analytical solution to the measurements. The parameters $h/\sqrt{D}$ via eq.(3) are plotted in Fig. 1 as the open circles. An evaluation via the time dependence of *water uptake* resulted in the triangles.

Measurements on water concentrations in silica heat treated in water vapour under saturation pressure were reported by Helmich and Rauch in [8]. In [7] we have compiled the most relevant data for the parameter $h/\sqrt{D}$ describing the time-dependency of water concentration at the free surface, eq.(3).
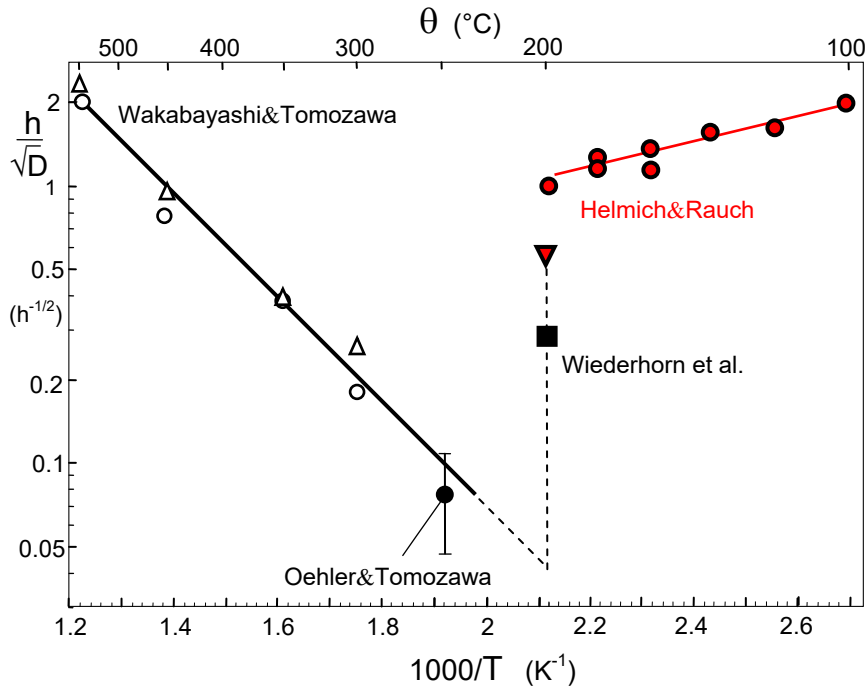

Fig. 1 Mass-transfer parameter $h/\sqrt{D}$ as a function of temperature; triangles: evaluation by fitting via water uptake measurements by Wakabayashi and Tomozawa [5]. Red circles and triangle: results from measurements at saturation pressure from Helmich and Rauch [8,9], square: from disk-curvature [9,10]. Black circle: based on measurements by Oehler and Tomozawa [1].

2.2 Computation of the parameters *h* and *h/D*

In the preceding considerations, only the parameter $h/\sqrt{D}$ has been determined that describes the time dependence of the surface water concentration. For the general solution of the diffusion problem, the ratio of mass transfer coefficient *h* and diffusivity *D* has to be known in eq.(1).

In order to compute h/D, we need the diffusivity *D* as a function of temperature and water vapour pressure. Figure 2a shows literature data of the diffusivity under 355 Torr water vapour by Davis and Tomozawa [11] as the black circles and the straight line. We fitted these results according to

$$D = A_D \exp\left(\frac{-Q_D}{RT}\right) \tag{4}$$

2

with $Q_D = 80.6$ [76.3, 85.0] kJ/mol and $\ln A_D = -13.64$ [−14.13,−13.15] cm^2/s. The numbers in brackets are 90%-Confidence Intervals.

For diffusivities in liquid water, Zouine et al. [12] (black line in Fig. 2b) give $Q_D = 72.3\pm2$ kJ/mol and $A_D = 7.6\times10^{-5}$ cm^2/s. Finally, the disk deformation measurements result in nearly the same data with a pre-factor that is increased by a factor of about 1.6 (see [7]), i.e. $Q_D = 72.3\pm2$ kJ/mol and $A_D = 12.2\times10^{-5}$ cm^2/s.
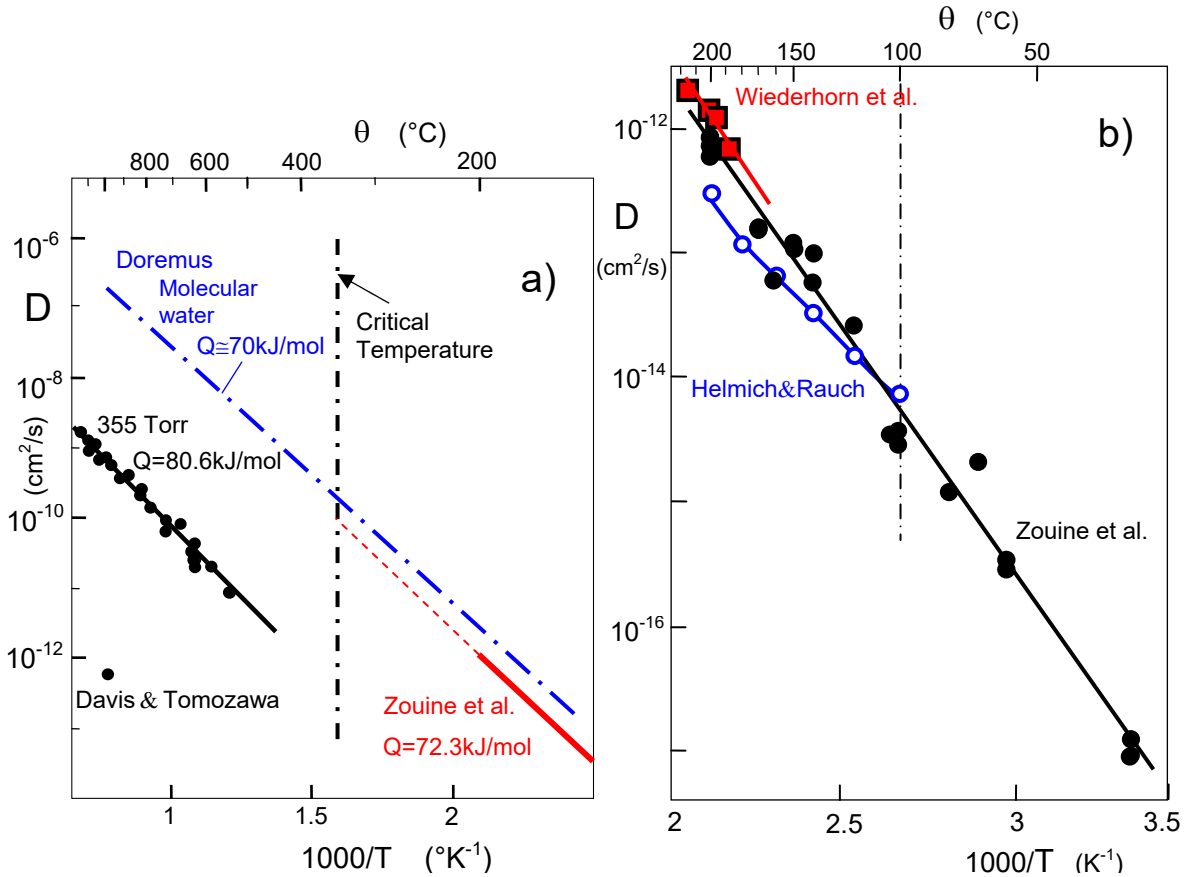

Fig. 2 a) Effective diffusivity for water in silica (black circles) at constant water vapour pressure of 355 Torr from Davis and Tomozawa [11], compared to effective diffusivities of water at saturation pressure (red line) and molecular water (blue line); b) diffusivities at saturation pressure, black: in liquid water from Zouine et al. [12], blue: in water vapour, by Helmich and Rauch [8], red: in water vapour by Wiederhorn et al. [10].

From the results of Fig. 1, the boundary parameter h is simply obtained from $h/\sqrt{D}$ via $h = (h/\sqrt{D})\times\sqrt{D}$. The parameter h/D necessary in eq.(2) is obtained via $h/D = (h/\sqrt{D})/\sqrt{D}$. Figure 3a represents the results for all data points in Fig. 1. The open symbols are measurements at constant pressure $p=355$ Torr, the solid ones represent data obtained under water saturation pressure. Whereas for the constant pressure data the parameter $h/\sqrt{D}$ in Fig. 1 varied strongly with temperature, the parameter h/D is within scatter nearly independent of temperature and can be expressed as

$$\frac{h}{D} \approx 1.33 \times 10^6 \ (SD = 2.85 \times 10^5)/\text{m} \qquad (5)$$

This value is indicated in Fig. 3b by the solid horizontal line. The dash-dotted lines represent the range of ±1 Standard Deviation (SD). Within the scatter, there is no temperature dependency of h/D visible.

Least-squares analysis of the straight lines in Fig. 3a provides Arrhenius-expressions

$$h = A_h \ \exp\left[-\frac{Q_h}{RT}\right] \qquad (6)$$

with A_h=0.221 m/h, Q_h=75.4 kJ/mol for the data at vapour pressure p=355 Torr, and A_h = 2.52 10^{-5} m/h, Q_h=17.3 kJ/mol (also compiled in Table 1) for saturated water vapour p=p_{sat}. The related straight lines are introduced in Fig. 3a.
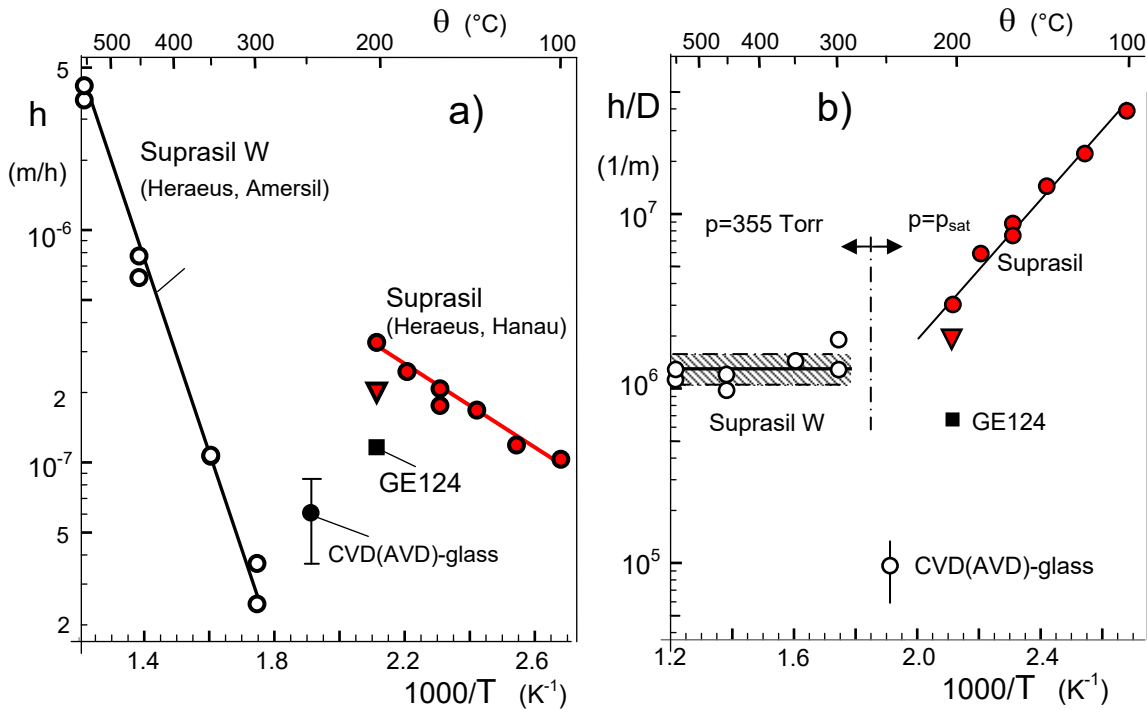

Fig. 3 a) Mass transfer coefficient h obtained from Figs. 1 and 2, straight lines according to eq.(6), b) parameter h/D, necessary for an evaluation of eq.(2).

2.3 Hydroxyl concentration at the silica surfaces

Recent investigations on silica surfaces show that silica is more reactive chemically at the surface than in the bulk, which may account for a very high but strongly localized hydroxyl concentration at the surface. In contrast to the SiO_2-structure in the bulk of silica, under-coordinated Si and O atoms occur at the free surface because of missing neighboured atoms.

These are more reactive so that when this surface is exposed to water vapour, water molecules react nearly instantaneously with the SiO_2 surface molecules to form SiOH as has been shown by molecular dynamic computations (see e.g. Mahadevan and Garofalini [13]).
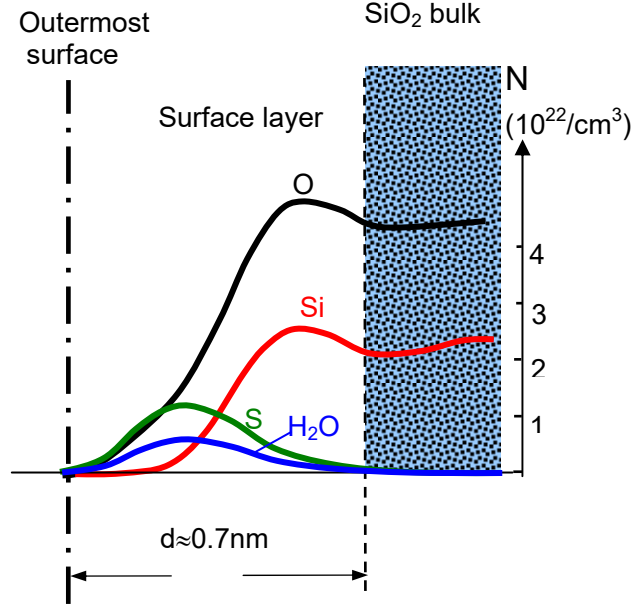

Fig. 4 At a free silica surface water reacts nearly instantaneously with under-coordinated silica species in a thin surface layer of about 0.7 nm thickness; curves according to Mahadevan and Garofalini [13], hydroxyl $S = [\equiv SiOH]$.

When the silica surface is exposed to a water vapour environment, additional water molecules are docked at the hydroxyl groups. Water molecules are trapped at the "free" ends of the surface molecules for a short while resulting in a dynamic equilibrium: water molecule coming in from the environment are then captured by the surface, while water released from the surface is free to diffuse deeper into the bulk as has been studied by computer modelling of the diffusion process [14,15,16].

The composition of a silica surface after contact with water molecules is illustrated in Fig. 4. The maximum S-concentration is $\approx 1.2 \times 10^{22}$ molecules/cm^3. Integrating the curves over the surface layer results in a total amount of

$$\frac{N_S}{A} = \int_0^\infty S\, dz = 3.8 / nm^2 \tag{7}$$

as is in agreement with Mahadevan and Garofalini [13] which report for the hydroxyls also $N_S/A = 3.8 \times 10^{22}/nm^2$.

The surface concentrations by Banerjee et al. [17] represent the average water amount in a thin volume of 10 nm thickness although the real surface layer is less than 1nm.

For this layer they report an average of 5.2×10^{20} S-molecules/cm^3. Zhuravlev [18] reports experimental results of $N_S/A=4.6$/nm^2 for a very large number of glass qualities. All these results are in good agreement.

3. Effect of surface layer on diffusivity

3.1 Diffusivity in the surface layer

The swelling strain results as

$$\varepsilon_v = \kappa \times S \ , \quad \kappa = 0.97 \tag{8}$$

(see e.g. [19]). In thin surface layers, the hydrostatic swelling stress is given as

$$\sigma_{sw,h} = \tfrac{1}{3}(\sigma_{sw,y} + \sigma_{sw,z}) = -\frac{2\,\varepsilon_v\,E}{9(1-\nu)} \tag{9}$$

On the other hand the diffusion depends on the hydrostatic stress term. The diffusivity for the case of stress-affected diffusion is for the swelling stresses given by the following equation [20]

$$D = D_0 \exp\left[\sigma_{sw,h}\frac{\Delta V_w}{RT}\right] \tag{10}$$

where D_0 denotes the value of the diffusivity in the absence of any stresses. T is the absolute temperature in K; ΔV_w is the activation volume for stress-enhanced diffusion and R is the universal gas constant. Since the swelling stresses are negative (compression), the diffusivity under strong swelling is strongly reduced.

3.2 Effect on the mass transfer coefficient

This fact was the basis for the simple model for reduced mass transfer at silica surfaces outlined in [21]

$$D = D_0 \exp\left[-\frac{2\times0.97\,S\,E}{9(1-\nu)}\frac{\Delta V_w}{RT}\right] \tag{11}$$

where D_0 results as the diffusivity in the absence of hydroxyl, i.e. for $S=0$. Equation (11) makes it clear that the diffusivity $D(1/T)$ must always fall with increasing $1/T$ regardless of the exact S-concentration of the thin surface layer. This is in agreement with the results from experimental data, represented by the equation (6).

The hydrostatic swelling stresses have been computed in [21] and are shown again by the left ordinate of Fig. 5a. Compressive hydrostatic stress reaches a maximum value of $\sigma_{sw,h} = -2.8\,\text{GPa}$. This value was computed in [21] with the effective volume $\Delta V_w \cong 16\,\text{cm}^3/\text{mol}$ as suggested by Lezzi et al. [22]. Figure 5b represents the related variation of the diffusivity.

Figure 6 schematically illustrates the consequences of the reduced diffusivity in the surface layer. In Fig. 6a, the distribution of the diffusivity along the depth coordinate is plotted once more. Figure 6b shows the water profile for a fixed time. The water concentration directly at the surface, C_0, is assumed generally to be constant only depending on the partial pressure of water in the environment.

Basic data	pressure	A_h (m/h)	Q_h (kJ/mol)
[5]	355 Torr	0.221	75.4
[8]	$p=p_{sat}$	2.52×10^{-5}	17.3

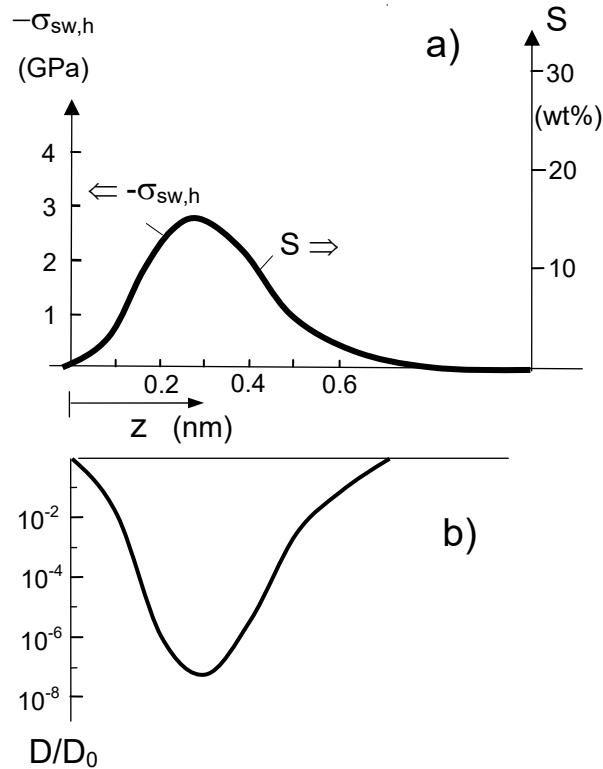**Table 1** Parameters of eq.(6) for Suprasil.

Fig. 5 Hydroxyl concentration (a) in weight percent, resulting in compressive hydrostatic swelling stresses (upper curve). The lower curve (b) shows the strongly reduced water diffusivity D, normalized on the diffusivity D_0 for stress-free silica at room temperature.
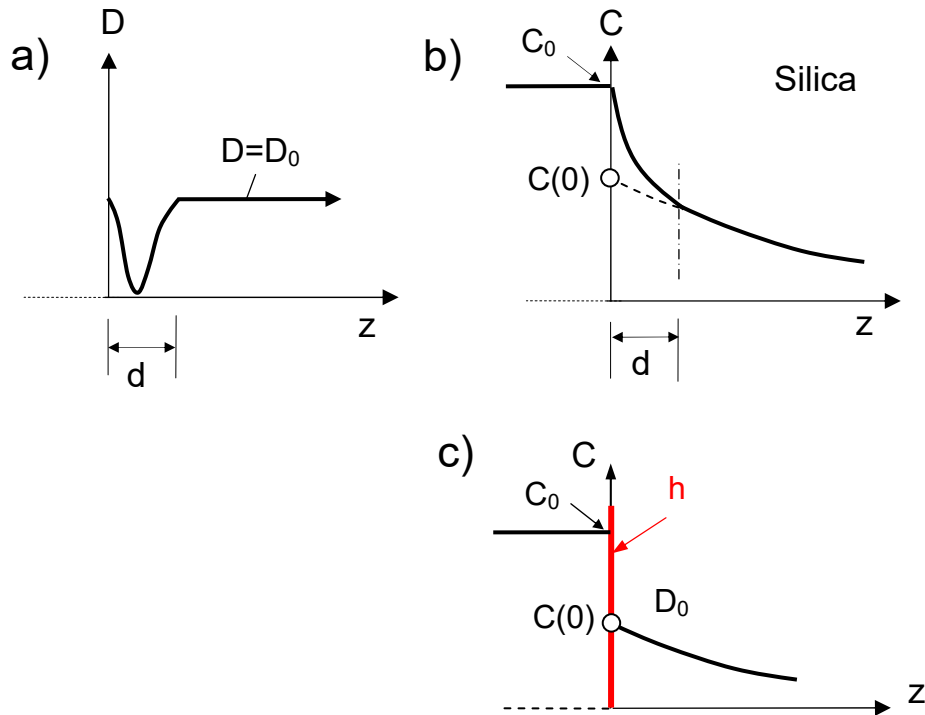
Fig. 6 a) Schematic representation of the diffusivity in the surface region, b) related water concentration profile, c) finite surface layer replaced by a surface with a finite mass transfer coefficient.

References

1 Oehler, A., Tomozawa, M., Water diffusion into silica glass at a low temperature under high water vapor pressure, J. Non-Cryst. Sol. **347** (2004) 211-219

2 R.H. Doremus, Diffusion of Reactive Molecules in Solids and Melts, Wiley, 2002, New York.

3 S.M. Wiederhorn, G. Rizzi, S. Wagner, M.J. Hoffmann, T. Fett, Diffusion of water in silica glass in the absence of stresses, J Am Ceram Soc. **100** (2017),3895–3902.

4 Carslaw, H.S., Jaeger, J.C. Conduction of heat in solids, 2nd ed. 1959, Oxford Press, London.

5 Wakabayashi, H., Tomozawa, M., Diffusion of water into silica glass at low temperature, J. Am. Ceram. Soc. **72** (1989), 1850-55.

6 T. Fett, G. Schell, C. Bucharsky, Mass Transfer of Water at Silica Surfaces - Extension of the data base to lower temperatures, Scientific Working Papers **189**, 2018, ISSN: 2194-1629, Karlsruhe, KIT.

7 T. Fett, G. Schell, C. Bucharsky, Interpretation of silica-disk-tests including the effect of limited mass transfer at the surface, Scientific Working Papers **196**, 2018, ISSN: 2194-1629, Karlsruhe, KIT.

8 M. Helmich and F. Rauch, "On the mechanism of diffusion of water in silica glass," *Glastech. Ber.* **66** [8] (1993), 195-200.

9 T. Fett, G. Schell, Water concentration and swelling stresses at silica surfaces derived from literature data - Estimation of mass-transfer coefficients, Scientific Working Papers **94**, 2018, ISSN: 2194-1629, Karlsruhe, KIT.

10 S. M. Wiederhorn, F. Yi, D. LaVan, T. Fett, M.J. Hoffmann, Volume Expansion caused by Water Penetration into Silica Glass, J. Am. Ceram. Soc. **98** (2015), 78-87.

11 Davis, K.M., Tomozawa, M., Water diffusion into silica glass: structural changes in silica glass and their effect on water solubility and diffusivity, J. Non-Cryst. Sol. **185** (1995), 203-220.

12 A. Zouine, O. Dersch, G. Walter and F. Rauch, "Diffusivity and solubility of water in silica glass in the temperature range 23-200°C," *Phys. Chem. Glass: Eur. J. Glass Sci and Tech. Pt. B*, **48** [2] (2007), 85-91.

13 T.S. Mahadevan, S.H. Garofalini, Dissociative chemisorption of water onto silica surfaces and formation of hydronium ions, J. Phys. Chem. C **112**(2008), 1507-1515.

14 Feuston, B.P., Garofalini, S.H., Water induced relaxation of the vitreous silica surface, J. Appl. Phys. **68**(1990), 4830-4836.

15 Leed, E.A., Pantano, C.G., Computer modelling of water adsorption on silica and silicate glass fracture surfaces, J. Non-Cryst. Sol. **325**(2003), 48-60.

16 Ma, Y., Foster, A.S., Nieminen, R.M., Reactions and clustering of water with silica surface, J. Chem. Phys. **122** 144709 (2005).

17 Banerjee J, Kim SH, Pantano CG. Elemental areal density calculation and oxygen speciation for flat glass surfaces using x-ray photoelectron spectroscopy. *J Non Cryst Solids* 2016; **450**: 185–193.

18 L.T. Zhuravlev, The surface chemistry of amorphous silica. Zhuravlev model, *Colloids and Surfaces, A: Physicochemical and Engineering Aspects* **173**(2000), 1-38.

19 T. Fett, K.G. Schell, S.M. Wiederhorn, Molar volume of SiOH estimated from swelling strains, International Journal of Applied Glass Science, **11** (2020), 608-611.

20 P.G. Shewmon, Diffusion in Solids, McGraw-Hill, New York, 1963.

21 T. Fett, G. Rizzi, K.G. Schell, C.E. Bucharsky, P. Hettich, S. Wagner, M. J. Hoffmann, Consequences of hydroxyl generation by the silica/water reaction Part I: Diffusion and Swelling, KIT Scientific Publishing, Karlsruhe.

22 P.J. Lezzi, Q.R. Xiao, M. Tomozawa, T.A. Blanchet, C.R. Kurkjian, Strength increase of silica glass fibers by surface stress relaxation: A new mechanical strengthening method, J. of Non-Crystalline Solids **379** (2013) 95–106.